

Creating Temporally Correlated High-Resolution Power Injection Profiles Using Physics-Aware GAN

Hritik Gopal Shah

Resiliency and Reliability Department
Eversource Energy, Hartford, CT, USA
hshah59@asu.edu

Behrouz Azimian, Anamitra Pal

School of Electrical, Computer, and Energy Engineering
Arizona State University, Tempe, AZ, USA
bazimian@asu.edu; Anamitra.Pal@asu.edu

Abstract— Traditional smart meter measurements lack the granularity needed for real-time decision-making. To address this practical problem, we create a generative adversarial networks (GAN) model that enforces temporal consistency on its high-resolution outputs via hard inequality constraints using a convex optimization layer. A unique feature of our GAN model is that it is trained solely on slow timescale aggregated power information obtained from historical smart meter data. The results demonstrate that the model can successfully create minutely interval *temporally-correlated instantaneous power injection profiles* from 15-minute *average power consumption information*. This innovative approach, emphasizing inter-neuron constraints, offers a promising avenue for improved high-speed state estimation in distribution systems and enhances the applicability of data-driven solutions for monitoring such systems.

Index Terms— Convex optimization layer, Deep generative adversarial networks, Scenario generation, Smart meters.

I. INTRODUCTION AND MOTIVATION

Distribution systems were once considered passive components of the grid due to the absence of generation within them. However, with the increasing installation of distributed energy resources (DERs), they are transforming from passive elements to active market-ready entities. At the same time, the inherent variability of DERs poses a significant challenge to the reliable operation of active distribution systems, necessitating an evolution of their monitoring infrastructure. In this regard, the introduction of advanced metering infrastructure (AMI) in the form of smart meters has ushered in a new era, furnishing additional measurement sources that significantly amplify the observability of distribution systems. Smart meter measurements primarily serve energy-related purposes, such as monthly billing calculations. Typically, their records capture *the average power consumption* over 15 or 60-minute intervals [1]. However, this aggregated reading is unable to capture the fast variations in *instantaneous power injection* values. More importantly, smart meters send data after a latency period that can range from *a few hours to a day* [2]. This means that smart meter measurements are not available for real-time decision-making, which limits their use for important applications such as high-speed distribution

system state estimation (DSSE). Note that the terms averaged and aggregated used in this paper refer to the same thing: power reported by smart meters over a given time interval.

Recently, it has been demonstrated that *learning-based methods* can enhance utilization of all available measurements in distribution systems by segregating the use of different time resolution data between offline training and real-time operation [2]-[4]. Historical AMI data can be employed in the offline training stage, thus overcoming the aforementioned limitations of smart meter measurements, while a limited set of high-speed sensors (e.g., supervisory control and data acquisition (SCADA) at feeder-head) can be used exclusively during real-time operation. The learning-based methods can provide fast and accurate state estimates for real-time unobservable distribution systems [5], while outperforming conventional methods that rely on pseudo-measurements achieved from load forecasting techniques [6].

An important component of these learning-based methods is the training database. This is because the scenarios present in the database must effectively represent the power injection variations occurring at the fast timescales. For creating such a database, one needs power injection profiles at a higher resolution than what AMI can provide. To address this practical problem, data-driven generative models can be employed to convert slow timescale measurements to fast timescale measurements, similar to the concept of *super-resolution* [7]. Super-resolution, a well-known theory in image processing, involves generating high-resolution images from low-resolution images. In power system applications, Liu et al. introduced super-resolution perception for processing smart meter data [8]. However, it introduced unrealistic details and oversmoothed the reconstructed high-resolution data. There is a growing body of literature that is employing generative adversarial networks (GAN) to create load profiles [9]. For instance, Song et al. proposed ProfileSRGAN, which aims to up-sample load profiles from low-resolution to high-resolution, thus restoring high-frequency components lost during the down-sampling process [10]. However, if the underlying physics of the system is ignored, the generated dataset can have huge variations for a specific time-period making them unrealistic. Thus, embedding knowledge of the system's physics into the learning model by incorporating appropriate constraints during training is crucial.

Constrained optimization techniques have gained significant attention in the training of deep learning models. While deep learning is often perceived as unconstrained, it is increasingly recognized that simple constraints can be effectively incorporated within deep learning procedures. Existing approaches for applying constrained optimization typically involve the use of penalty terms in the loss function to enforce soft boundary constraints [11]. However, these approaches only penalize infeasibility without guaranteeing feasibility. Alternatively, hard constraints can be implemented by either processing the output of an unconstrained model [12], or designing a model that inherently produces feasible predictions [13]. Most recent works have investigated differentiable optimization layers for neural networks, as such approaches could be used to directly enforce the constraints, e.g., by projecting neural network outputs onto a constraint set using quadratic programming layers in the case of linear constraints [14], or convex optimization layers in the case of general convex constraints [15].

A. Summary of Our Contributions

In this work, we introduce a novel GAN model that incorporates hard inequality constraints into its generator network using CVXPY (convex optimization) layers. The primary objective is to generate high-resolution temporally-correlated datasets at fast timescales effectively. By integrating these hard inequality constraints into the generator network, we establish "*inter-neuron constraints*" within the neural network. These constraints govern how the neurons or units within a specific hidden layer interact with each other while contributing to the overall data generation process.

The second unique feature of our approach is that we only use slow timescale average power consumption information obtained from historical smart meter data for training. This design choice makes our model applicable to scenarios where access to fast timescale or high-resolution data is limited or restricted. The results of our study demonstrate that the proposed GAN model, when trained using 15-minute interval (slow timescale) *aggregated* power information from smart meters, can successfully generate minutely interval (high resolution) *instantaneous* power injection values. Furthermore, these generated data exhibit statistical realism and temporal consistency, making them suitable inputs for applications such as high-speed DSSE. The main contributions of our work are summarized below:

- 1) Embedding inter-neuron constraints for neurons present in the generator network of the GAN through incorporation of CVXPY layer.
- 2) GAN-based generation of temporally-correlated high-resolution power injection profiles from slow timescale average power consumption data from smart meters.

II. BASIC GAN MODEL

GAN is made up of two neural networks that compete against each other. The first neural network is known as the *generator*, which creates synthetic samples, while the second neural network is known as the *discriminator* (or critic) that distinguishes between the real and generated samples [16]. The primary goal of a GAN is to generate new statistically similar (but not identical) samples for an existing (real) dataset by first

learning the distribution of the real dataset, and then mapping it to a separate latent space. The initial focus is on optimizing the discriminator D , given the generator G . The training process for the discriminator entails minimizing the cross-entropy loss, which is formulated as shown below [17]:

$$\text{Loss}(D) = -\frac{1}{2} E_{r \sim p_{\text{data}}(r)} [\log D(r)] - \frac{1}{2} E_{f \sim p_f(f)} \left[\log \left(1 - D(G(f)) \right) \right] \quad (1)$$

where, r is sampled from real data with probability $p_{\text{data}}(r)$, f is sampled from the prior distribution $p_f(f)$ such as uniform or Gaussian, and E denotes the expectation operation. The training data consists of two parts: one obtained from the real data distribution $p_{\text{data}}(r)$, while the other obtained from the generated data distribution $p_G(r)$. Given the generator G , we minimize (1) to obtain the optimal solution. Equation (1) can be reformulated as shown below:

$$\begin{aligned} \text{Loss}(D) &= -\frac{1}{2} \int_r p_{\text{data}}(r) \log D(r) dr - \\ &\frac{1}{2} \int_f p_f(f) \log \left(1 - D(G(f)) \right) df \\ &= -\frac{1}{2} \int_r [p_{\text{data}}(r) \log D(r) + p_G(r) \log(1 - D(r))] dr \quad (2) \end{aligned}$$

where, $D(r)$ denotes the probability of r being sampled from the real data rather than the generated data. Now, for any $(a, b) \in \mathbb{R}^2 \setminus \{0,0\}$ and $c \in [0,1]$, the expression: $-a \log(c) - b \log(1 - c)$, achieves its minimum value at $c = a/(a + b)$. Hence, given generator G , the objective function given in (2) achieves its minimum value at:

$$D_{G(r)}^* = \frac{p_{\text{data}}(r)}{p_{\text{data}}(r) + p_G(r)} \quad (3)$$

From the optimal solution shown in (3), it can be realized that the discriminator of the GAN estimates the ratio of two probability densities. When the input data is from the real data r , the discriminator strives to make $D(r)$ approach one. Conversely, if the input data is from the generated data $G(f)$, the discriminator strives to make $D(G(f))$ approach zero, while the generator G tries to make it approach one. Since this is a zero-sum game between G and D , the loss function of G is the negative of the loss function of D ; i.e., $\text{Loss}(G) = -\text{Loss}(D)$. Therefore, the overall optimization formulation of the GAN can be expressed as a two-player minimax game with value function $V(G, D)$, as shown below:

$$\begin{aligned} \min_G \max_D V(G, D) &= \\ E_{r \sim p_{\text{data}}(r)} [\log(D(r))] - E_{f \sim p_f(f)} [\log(1 - D(G(f)))] \quad (4) \end{aligned}$$

Finally, we must train the generator G to minimize $\log(1 - D(G(f)))$. Here, we can use an alternate training method. First, we fix G and optimize D to maximize the discrimination accuracy of D . Then, we fix D and optimize G to minimize the discrimination accuracy of D , as seen in (4). This process alternates, with the global optimal solution achieved only when $p_{\text{data}} = p_G$. Note that during the training process, the parameters of the discriminator D undergo empirical updates multiple times before the parameters of the generator G are updated once. This sequential updating strategy contributes to the convergence of the GAN and the attainment of a more effective generative model.

III. PROPOSED PHYSICS-AWARE GAN

Without any loss of generality, it can be assumed that the slow timescale aggregated smart meter data are m times slower than the fast timescale data, say, coming from the SCADA system. Since the SCADA system is not deployed throughout the distribution system to observe it at high-speeds, the goal is to *create realistic statistically accurate SCADA-like data using smart meter measurements*. In the proposed approach, we use historical average power data from smart meters to train a GAN with physics-based conditions applied as inter-neuron constraints inside the generator network through the CVXPY layer. The generator produces fast timescale synthetic profiles of size $m \times n$ from the convex optimization layer, which are then aggregated row-wise to generate n smart meter-like measurements for comparison by the discriminator.

A. Generator Block of Proposed GAN

The proposed GAN (see Fig. 1) is trained on physics-based constraints by incorporating a CVXPY layer after the dense layers of the generator's deep neural network. This creates an end-to-end trainable network that enables addition of inter-neuron constraints. The CVXPY layer is a convex optimization model that trains the GAN with user-defined inputs. Note that the CVXPY layer is the penultimate layer of the generator. After this layer, we have the *Aggregator function* layer, which is non-trainable. This layer performs the average operation on the outputs of the CVXPY layer to match the generator's outputs with the dimensions of the slow timescale AMI data. Finally, the aggregated data is sent to the discriminator of the proposed GAN. The input of the generator is a noise vector that is sampled from a uniform distribution.

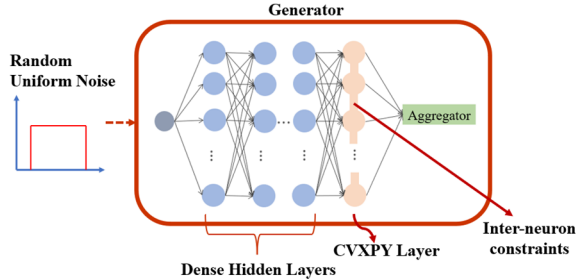


Figure 1. Proposed generator model

B. CVXPY Layer

CVXPY layer is a differentiable optimization layer [15]. Optimization layers add domain-specific knowledge or learnable hard constraints to machine learning models. They solve convex, constrained optimization problems of the form:

$$x(\theta) = \arg \min_x J(x, \theta) \quad (5)$$

$$\text{s. t. } l(x; \theta) \leq 0$$

$$h(x; \theta) = 0$$

with parameters θ , objective J , and constraint functions l and h doing end-to-end learning through them with respect to θ . These constraints are vital in scenarios where the desired outcomes of a model must satisfy particular conditions.

In our case, the CVXPY layer plays a crucial role in optimizing the generator's neural network as it ensures creation of synthetic data that adheres to physics-based constraints via

inter-neuron constraints. The imposition of such constraints elevates the generator's capability from merely mimicking data patterns to actively conforming to the intricate dynamics of the system. The proposed CVXPY layer solves a parameterized convex problem in the forward pass to produce a solution. In the backward pass, it computes the derivative of the solution with respect to the parameters. Through this process, the CVXPY layer learns a parameterized objective function and multiple hard constraints from data that are initially unknown to the model. The details of the objective function and constraints is provided in (7) of Section III.D.

C. Discriminator Block of Proposed GAN

The discriminator is a vanilla deep neural network with dense layers and a Sigmoid activation function as its output. It acts similar to a switch (see Fig. 2): the discriminator is first trained with actual smart meter data, and then it is trained with the fake dataset created from the generator. At the end, it outputs a continuous probability score indicating the likelihood that a given input is real or fake.

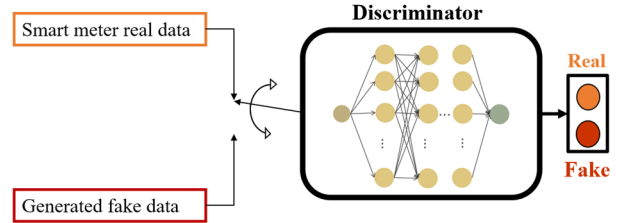


Figure 2. Discriminator network

D. Overall Structure of the Proposed GAN

The GAN created here is not only a more generic method to learn distributions without having strong assumptions but also it allows us to learn a distribution when the samples are not directly observable. The objective function of the proposed GAN model is a two-player minimax game given by:

$$\min_G \max_D V(G, D) = E_x[\log(D(x))] - E_z[\log(1 - D(G(\sum CVXPY(z))))] \quad (6)$$

Equation (6) is obtained by modifying the objective function of the basic GAN model (see (4)) by including the CVXPY and Aggregator function layers inside the GAN framework. The final structure is shown in Fig. 3. Both generator and discriminator have two hidden (dense) layers with 128 neurons in each layer. Batch normalization and dropout rate of 0.3 are used in these layers. The third hidden layer of the generator is the CVXPY layer, which contains 15 neurons and is followed by an Aggregator as the output layer, which has non-trainable parameters. Note that this structure corresponds to a SCADA availability of one sample every minute, while smart meter data was assumed to be available for 15 aggregated samples; i.e., $m = 15$.

To learn the fast timescale power injection distribution using the smart meter measurements, we made the following modifications. Instead of generating *one* sample from the CVXPY layer, we generated 15 samples from it (since $m = 15$) and averaged them to imitate a measurement from smart meters at each slow timescale interval. Next, to embed temporal correlations into our data generation process, the following constraints were added in the CVXPY layer:

$$z^* = \underset{z}{\operatorname{argmin}} \sum_{i=1}^m ((z_i - a_i)_i)^2 \quad (7.1)$$

$$(1 - k_1)L \leq z_i \leq (1 + k_2)U \quad (7.2)$$

$$(1 - k_3)z_{i-1} \leq z_i \leq (1 + k_3)z_{i-1} \quad (7.3)$$

Equation (7.1) minimizes the difference between the input (a_i) to the CVXPY layer and the output (z_i) for each neuron present in this layer, while (7.2) and (7.3) account for the temporal correlation between the generated high-resolution samples. The bounds on the maximum difference (in kW) that high resolution data can have from the minimum and maximum aggregated historical smart meter data are set in (7.2), while (7.3) limits abrupt increments or decrements from one sample to the next. L (U) is the minimum (maximum) average power consumption value recorded in historical smart meter data, and k_1, k_2, k_3 are appropriate constants. Equation (7) ensures that the proposed GAN produces temporally-correlated high-resolution power injection profiles.

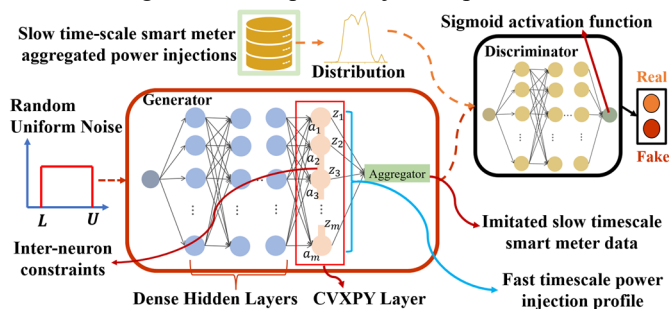


Figure 3. Proposed physics-aware GAN model

IV. SIMULATION RESULTS

We used the power injection data from the Pecan Street database [18] for training our GAN. The load-level measurements occurring at minutely and 15-minute intervals from this database were employed for our analysis. To increase efficacy of the deep learning model, samples must be selected from historical data with similar features, such as same season and hour of the day. Therefore, for each load of the database, we selected power injection data from June 1st through August 31st of 2018 between 12 Noon and 1 PM. The GAN was then trained using these samples.

We now used the generator of the trained GAN to create multiple temporally-correlated instantaneous high-resolution power injection profiles for the loads in the Pecan Street database. To validate the profiles, we produced samples that imitated smart meter observations from the generator and compared their cumulative distribution function (CDF) with the CDF of the actual smart meter readings obtained directly from the database. Fig. 4 shows the CDFs for a particular load. It is clear from the figure that they are comparable. A minor discrepancy between the real and generated datasets occurs near the tail-end; it can be addressed by additional fine-tuning of the constraints in the CVXPY layer.

Note that although the generator produces outputs at the slow timescale rate of one sample per 15 minutes (i.e., the output of the Aggregator layer in Fig. 3), the fast timescale measurements at minutely basis, namely z , are available at the output of the CVXPY layer (penultimate layer). This output is

the required SCADA-like data that the proposed approach can produce at every location where a smart meter is placed. Essentially, this makes every load-with-smart meter observable at SCADA timescales using only AMI data.

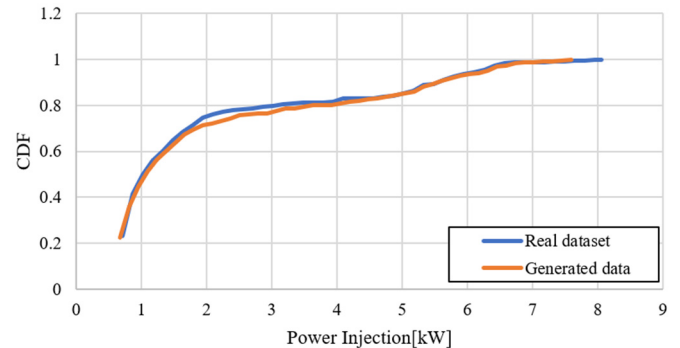


Figure 4. CDF comparison. Blue curve is the CDF of smart meter data; Orange curve is the CDF of imitated measurements from learned distribution

Next, we compare the proposed physics-aware GAN with the traditional GAN developed in [3]. This comparison is meant to highlight the significance of the CVXPY layer in enforcing essential inter-neuron constraints that play a pivotal role in the *fidelity* of the generated data. The method proposed in [3] demonstrates high degree of similarity in the *aggregated values*, reaffirming the overall effectiveness of using GAN in capturing statistical characteristics of smart meter data (similar to what was shown in Fig. 4). However, a significant difference emerges when we delve into the fast timescale measurements, as the traditional GAN framework is unaware of the power system physics-based constraints. This is elaborated below.

For the same load (that was used for Fig. 4), it was observed that for the season and hour that were the focus of this study, the minutely power injection data varied between 0 and 12.5 kW, while the aggregated 15-minute smart meter data varied between 0.55 and 8.5 kW. Therefore, we chose $k_1 = 100\%$, $k_2 = 47\%$, $L = 0.55$, and $U = 8.5$. Furthermore, it was observed that a valid minutely measurement was never more than 50% of its predecessor; as such, we put $k_3 = 50\%$. The proposed physics-aware GAN was able to account for these power system realities through the CVXPY layer, while the traditional GAN could not. The difference is observed in Fig. 5, which shows minutely samples for a period of 15 minutes. As the traditional GAN structure is not aware of the physical constraints present in the power injection profiles, it often outputs values that are outrageous (e.g., 207% difference between two consecutive generated samples). However, the proposed GAN generates much more reasonable (realistic) values by enforcing the physical constraints during high resolution sample generation.

To further evaluate the performance of our method in comparison to the traditional GAN, we analyzed a dataset consisting of 500 synthetic load profiles, each comprising a minutely sequence of 15-minute interval values. This allowed us to calculate the percentage increase or decrease between two consecutive minutes over a statistically large dataset. The key differences between the two GANs are readily apparent in Table I. For the proposed physics-aware GAN, the maximum percentage increase or decrease for any two consecutive minutes within each 15-minute time frame consistently

remained at or below 50% (see second column). This finding attests to the efficacy of our approach in enforcing the constraint between consecutive time intervals via the CVXPY layer. Conversely, for the traditional GAN, the percentage increase or decrease for two consecutive time frames could be extremely large (e.g., 8000%) resulting in abrupt changes in the generated consecutive power injection values, which is not realistic. In addition, the third column in Table I indicates that for the traditional GAN, we do not have any control on the maximum value generated for high resolution power injections (it went up to 14.5 kW in our simulations), while by adding the CVXPY layer we were able to limit the maximum value for generated high-resolution power injections to 12.5 kW (which matches with the limits of the minutely data). This comparative assessment strengthens our argument for the incorporation of inter-neuron constraints via the CVXPY layer as a promising avenue for advancing the realism of synthetic data.

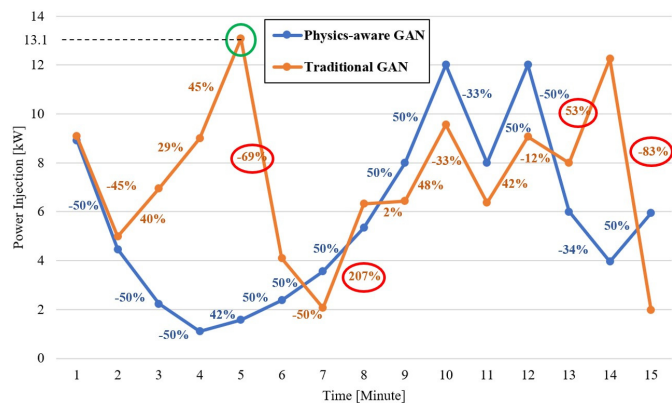


Figure 5. A high-resolution instantaneous power injection profile with and without CVXPY layer. Numbers on each line segment show the percent change for two consecutive samples. Green circle shows violation of (7.2) and red circles show violation of (7.3) for the traditional GAN

Table I. Maximum percentage change for two consecutive samples and maximum instantaneous value for 500 high-resolution power injection profiles

	Maximum decrease/increase [%]	Maximum power injection [kW]
Traditional GAN	8000	14.5
Physics-aware GAN	50	12.5

V. CONCLUSION

In this work we proposed a novel method based on GAN for augmenting the smart meter dataset and generating SCADA-like fast timescale measurements that currently do not exist in the distribution system. The generated data can be used for high-speed DSSE, even when the system is nominally unobservable due to lack of SCADA penetration.

By embedding convex optimization layers into the proposed GAN framework, we were able to create datasets that conform to specific constraints that were previously impossible to achieve. This new methodology holds great promise for various applications that require high-quality datasets with specific domain knowledge embedded inside the training process. This approach opens up new possibilities for the development of more robust and accurate machine learning models that can handle complex power system tasks. Our future endeavors will expand upon this work by focusing on

generating higher-resolution instantaneous power injection profiles with both temporal as well as spatial correlations.

DISCLAIMER

The author(s) of each article appearing in this article is/are solely responsible for the content thereof; the publication of an article shall not constitute or be deemed to constitute any representation by Eversource Energy that Eversource Energy has reviewed, approved or endorsed the article content or that the data presented therein are correct or sufficient to support the conclusions reached or that the experiment design or methodology is adequate.

REFERENCES

- [1] Advanced metering infrastructure and customer systems. Sept 2016. U.S. Department of Energy. [Online]. Available: https://www.energy.gov/sites/prod/files/2016/12/f34/AMI%20Summary%20Report_09-26-16.pdf
- [2] B. Azimian, R. S. Biswas, A. Pal and L. Tong, "Time synchronized state estimation for incompletely observed distribution systems using deep learning considering realistic measurement noise," in *Proc. IEEE Power & Energy Soc. General Meeting*, Washington, DC, USA, pp. 1-5, 2021.
- [3] K. R. Mestav and L. Tong, "State estimation in smart distribution systems with deep generative adversary networks," in *Proc. IEEE Int. Conf. Commun., Control, Comput. Technol. Smart Grids (SmartGridComm)*, Beijing, China, 2019.
- [4] B. Azimian, R. S. Biswas, S. Moshtagh, A. Pal, L. Tong and G. Dasarathy, "State and topology estimation for unobservable distribution systems using deep neural networks," *IEEE Trans. Instrum. Meas.*, vol. 71, pp. 1-14, Apr. 2022.
- [5] B. Azimian, S. Moshtagh, A. Pal, S. Ma, "Analytical verification of deep neural network performance for time-synchronized distribution system state estimation," *J. Modern Power Syst. Clean Energy*, in press.
- [6] K. R. Mestav, J. Luengo-Rozas and L. Tong, "Bayesian state estimation for unobservable distribution systems via deep learning," *IEEE Trans. Power Syst.*, vol. 34, no. 6, pp. 4910-4920, Nov. 2019.
- [7] K. Nasrollahi, and T. B. Moeslund, 'Super-resolution: A comprehensive survey', *Mach. Vision Applicat.*, vol. 25, no. 6, pp. 1423–1468, 2014.
- [8] G. Liu, J. Gu, J. Zhao, F. Wen, and G. Liang, 'Super resolution perception for smart meter data', *Information Sciences*, 526, pp. 263–273, 2020.
- [9] D. Dalal, M. Bilal, H. Shah, A. I. Sifat, A. Pal, and P. Augustin, "Cross-correlated scenario generation for renewable-rich power systems using implicit generative models," *Energies*, vol. 16, no. 4, pp. 1-20, Feb. 2023.
- [10] L. Song, Y. Li and N. Lu, "ProfileSR-GAN: A GAN based super-resolution method for generating high-resolution load profiles," *IEEE Trans. Smart Grid*, vol. 13, no. 4, pp. 3278-3289, Jul. 2022.
- [11] M. Raissi, P. Perdikaris, and G. E. Karniadakis, "Physics-informed neural networks: A deep learning framework for solving forward and inverse problems involving nonlinear partial differential equations," *J. Comput. Physics*, 378, pp. 686–707, 2019.
- [12] C.-H. Jiang, K. Kashinath, Prabhat, and P. Marcus, "Enforcing physical constraints in CNNs through differentiable PDE layer," *Int. Conf. Learning Representations*, Feb. 2020.
- [13] Z. Long, Y. Lu, and B. Dong, "PDE-net 2.0: Learning PDEs from data with a numeric-symbolic hybrid deep network", *J. Comput. Physics*, 399, pp. 108925, 2019.
- [14] B. Amos, J. Z. Kolter. "OptNet: Differentiable optimization as a layer in neural networks" *Int. Conf. Machine Learning*, pp. 136-145, 2017.
- [15] A. Agrawal, B. Amos, S. T. Barratt, S. P. Boyd, S. Diamond, and J. Z. Kolter. "Differentiable convex optimization layers." *Advances in 32nd Neural Information Processing Systems (NeurIPS)*, 2019.
- [16] I. J. Goodfellow et al., "Generative adversarial networks," *Commun. ACM*, vol. 63, no. 11, pp. 139-144, Oct. 2020.
- [17] K. Wang, C. Gou, Y. Duan, Y. Lin, X. Zheng, and F. Wang, "Generative adversarial networks: introduction and outlook," *IEEE/CAA J. Automatica Sinica*, vol. 4, no. 4, pp. 588–598, Jan. 2017.
- [18] Pecan Street Dataport. [Online]. Available: <https://dataport.pecanstreet.org/> [Accessed: 1- Nov- 2023].